

Polymer Chemistry

Accepted Manuscript



This is an *Accepted Manuscript*, which has been through the Royal Society of Chemistry peer review process and has been accepted for publication.

Accepted Manuscripts are published online shortly after acceptance, before technical editing, formatting and proof reading. Using this free service, authors can make their results available to the community, in citable form, before we publish the edited article. We will replace this *Accepted Manuscript* with the edited and formatted *Advance Article* as soon as it is available.

You can find more information about *Accepted Manuscripts* in the [Information for Authors](#).

Please note that technical editing may introduce minor changes to the text and/or graphics, which may alter content. The journal's standard [Terms & Conditions](#) and the [Ethical guidelines](#) still apply. In no event shall the Royal Society of Chemistry be held responsible for any errors or omissions in this *Accepted Manuscript* or any consequences arising from the use of any information it contains.

Polymeric Charge Storage Electrets for Nonvolatile Organic Field Effect Transistor Memory Devices

Ying-Hsuan Chou,^{†a} Hsuan-Chun Chang,^{†a} Cheng-Liang Liu^{*b} and Wen-Chang Chen^{*a}

^a Department of Chemical Engineering, National Taiwan University, Taipei 10617, Taiwan.

E-mail: chenwc@ntu.edu.tw

^b Department of Chemical and Materials Engineering, National Central University, Taoyuan, 32001 Taiwan. E-mail: clliu@ncu.edu.tw

[†]Y.-H. Chou and H.-C. Chang equally contribute to this work.

Abstract

In this review, we present the effects of chemical structure and composition of polymer or composite electrets on tuning the memory characteristics of the nonvolatile organic field effect transistor (OFET) memory devices, including surface polarity, π -conjugation length, architecture, donor-acceptor strength, and interface energy barrier. The recent progress towards developing in polymer-based charge storage electret are highlighted in order to provide insight on understanding the operation mechanism and molecular design-memory properties relationship, as well as improving overall performance of OFET memory devices.

1. Introduction

Nonvolatile memory devices based on organic field-effect transistors (OFET) architecture have attracted extensive research interest since they exhibit not only the unique benefits of low cost, light-weight, and flexible advantages alternative to the Si-based memory, but also non-destructive read-out and manufacturing compatibility with integrated circuits composed of OFET.¹⁻⁸ Transistor memories are prepared from the arrays of memory elements in which OFET cells involve one additional charge storage layer between the gate contact and organic semiconductor channel. Every memory cell contains one transistor allowing to store at least one bit through an additional electric field (voltage bias or pulse) applied at the gate contact and the charge distribution in the channel current flow of the OFET devices can be modulated. The charge can be stored within the bulk of dielectric film or at the interface between the gate dielectric and semiconducting channel.

In general, OFET memories are mainly divided into three categories based on the charge storage and polarization methods of the dielectric layer²: (1) floating-gate OFET memories; (2) polymer electret-based OFET memories; (3) ferroelectric OFET memories. A polymer electret, one kind of dielectric materials, exhibit a quasi-permanent electric field caused by trapping the electrostatic charges.¹⁻⁴ It has been recognized that memory functionalities resulted from the channel conductance modulation by trapped charges inside the polymer electret upon applying programming (PGM) or erasing (ERS) gate voltage (V_g), and the charge

storage capability is extensively determined by the chemical nature. Besides, electret materials are also meanwhile used in a wide variety of applications including filter, sensors, power generator, and transducer, etc.⁹ The utilization of polymeric charge storage electret as a reversible charging dielectric is a simple and effective strategy toward high performance nonvolatile OFET memories where the bistable or multistable states in the operation are reproducibly demonstrated through the hysteresis sweep or shift of the threshold voltage (V_g) in current (I)-voltage (V) characteristics. In the present review, we focus on the representative organic polymers and composites as the charge storage electrets in OFET memory devices and correlate the relationships between chemical structures, morphology, charge transport and memory characteristics.

2. Operation principle of OFET memory devices

The basic architecture of organic transistor-type memory device is consisted of three-terminal (source, drain, and gate) OFET with one additional polymer electret layer between the organic semiconductor and control dielectric, as shown in Fig. 1(a). For the OFET based on p-type semiconductor (for example, pentacene), the application of a sufficiently high negative gate voltage induces the accumulation region. The injected hole conducting channel within the organic semiconductor film between source and drain electrode can operate at the accumulation mode. Typically, OFET are characterized by the

drain current (I_d) vs V_g and I_d vs drain voltage (V_d), called the transfer and output curve, respectively. For the curve of $I_d^{1/2}$ vs V_g , its slope is linearly proportional to the carrier mobility (μ). Threshold voltage (V_{th}), defined as the V_g for which there is no space charge in the organic film, is the intercept from the extrapolating the curve with voltage axis. The trapped charges in the chargeable polymer dielectric vary the distribution of the carriers in the semiconducting channel, thus resulting in changes in V_g of the memory devices in relation to the programming or erasing operation. As a result, the digital “0” and “1” signals in one bit are determined by applying a read voltage (V_{read}) to the gate between the erasing and programming operations in order to verify the representing low and high I_d region for the erased and programmed states, respectively. Several parameters are used to determine the OFET memory device characteristics including memory window, memory ratio, retention and endurance ability. The V_g shift between PGM and ERS states is defined as memory window (Fig. 1(a)), one of the most important parameters on the OFET memory for distinguishing the information storage level. The memory sensing margin, memory ratio (Fig. 1(b)), is given by the I_d difference between programmed and erased states at a fixed of V_{read} (typically near 0 V for the purpose of non-destructive reading). Retention is a metric used to judge the ability of transistor memory device to preserve the programming/erasing states without losing the trapped charges through the leakage path over time (Fig. 1(c)). Therefore, it is an important reliability issue and at minimum 10^4 s is expected. The polymer electret maintains the ability

to collect or release the amount of charges in each programming/erasing cycle if the high switching endurance of repeatable 100 cycles or greater can be achieved (Fig. 1(d)). Non-volatility implies long charge retention and the data must be stored in a device cell after many reading/programming/erasing cycles.

The basic operation of nonvolatile p-type transistor memory device is depicted in Fig. 2. In the beginning, the flat band diagram of the p-type device junction implies that no charge exists in the semiconductor (Fig. 2(a)). As the positive/negative bias applied on the gate above a specific range, electrons/holes are stored in the polymer electret layer by PGM (Fig. 2(b))/ERS (Fig. 2(d)) operation. Then, they move back to the channel or be recombined with charges of opposite polarities through the reverse voltage bias (corresponding to ERS (Fig. 2(c))/PGM (Fig. 2(e)) operation). A nonvolatile transistor memory means that the accumulated charges are still trapped in the polymer dielectric and information can be maintained even after the V_g is removed.

3. Polymer electrets for nonvolatile memory devices.

The storage capability is determined by the chemical structures, composite ratio and morphology of charge trapping electrets, as analyzed by the following. Tables 1-3 provide a summary of OFET memory characteristics for representative polymers and their composites electret materials. The following section categorizes the examples based on the single component (pendent polymers¹⁰⁻²⁵ and donor-acceptor polyimides²⁶⁻²⁹) or polymer

composites³⁰⁻³⁵ as polymeric electrets and analysis how memory properties are impacted.

3.1 Side-chain polymer electrets with pendent functional groups

3.1.1 Effect of hydrophobic/hydrophilic side-chain

An overview of pendent polymer electrets used in OFET memories is given in Fig. 3 and the memory properties are summarized in Table 1. Katz et al. reported OFET with both p-type 1,4-bis(5-phenyl-2-thienyl)benzene (PTPTP) and n-type N,N'-bis(1H,1H-perfluorooctyl) naphthalene-1,4,5,8-tetracarboxylic diimide (F15-NTCDI) organic semiconductors, using two hydrophobic polymers, poly (4-methylstyrene) (**P1**) and cyclic olefin copolymer (**P2**) as polarized gate insulators.¹⁰ Adjustment of V_{th} from the accumulation mode to either zero or depletion mode was accomplished by applying a depletion voltage to the gate electrode prior to device operation, but need a relatively long time (at least 10 min) to switch the device. Singh et. al. introduced polyvinyl alcohol (PVA; **P3**) electret as the gate insulator for fullerene (PCBM) based OFET memory device,¹¹ which featured a hysteresis in the transfer curves with a memory window of ~14 V and a very long retention up to 15 h. Besides, p-type lead phthalocyanine (PbPc)-based OFET memory with the **P3** electret also showed the memory window increased with an enhanced magnitude of V_g or V_d , with reproducible endurance switching cycles and data retention of more than 5 h.¹²

Baeg et al. reported that an OFET nonvolatile memory devices based on pentacene using poly(α -methylstyrene) (P α MS; **P4**) electret,¹³ which showed a relatively short switching time

of less than 1 μs , a long retention time of more than 100 h, a high memory ratio of 10^5 and a large memory window of ~ 90 V. Later, they discovered that both the degree of memory window and retention time are inversely proportional to the degree of hydrophobicity and polarity of the polymer electrets using the following electret, poly(α -methylstyrene) (P α MS; **P4**), polystyrene (PS; **P5**), and poly(2-vinylnaphthalene) (PVN; **P6**) with those of hydrophilic and polar polymers (**P3**, poly(4-vinylphenol) (PVP; **P7**), and poly(2-vinylpyridine) (PVPyr; **P8**)).¹⁴ It was seen that non-polar and hydrophobic polymers were more superior chargeable dielectrics since the transferred and trapped charges in hydrophilic and polar pendent polymers rapidly dissipated through the conducting pathway derived from the remaining moistures, ions and impurity. Lim et al. studied the OFET memory using the **P7** electret mixed with various amounts of crosslinkable methylated poly (melamine-co-formaldehyde) (MMF).¹⁵ The device showed a large hysteresis curve at a low MMF content but only a small hysteresis at a high MMF content, which was strongly related to the hydroxyl groups in the polymeric dielectrics. Guo and coworkers further confirmed that the orientation of the hydroxyl groups in the **P3** gate electret significantly affected the hysteresis of transfer characteristics under the forward and backward scan.¹⁶ Debucquoy et al. also studied a similar pentacene/**P4** electret device and electron trapping in **P4** was only possible when the pentacene was ambipolar.¹⁷ They suggested that the hydrophilic and polar polymers had a poor memory effect since these dielectrics containing hydroxyl groups could

induce electron traps to hamper the electron accumulation in pentacene. Amorphous poly(methyl methacrylate) (PMMA; **P9**) was also used for nonvolatile memory device as compared with the **P3** electret with stronger polar groups.¹⁸ Based on the results from the retention and endurance testing, the **P9** electret-based devices were much more stable and reliable than those of the **P3**-based devices, although the **P3** electret-based devices had a relatively larger memory window. They proposed that large amount of shallow-type traps in the **P3** devices was created due to the rough interface and the strong polar OH groups. The more free volume vacancies within the **P9** layer provided a possible origin for the long lifetime deep-type traps in the memory devices. It suggests that nonvolatile memory properties strongly depend on the hydrophilic/hydrophobic pendent group of a charge storage layer and its interface with the semiconducting layer.

3.1.2 Effect of π -conjugated length in side-chain moieties

Polymer pendent with precisely defined π -conjugated moieties (see Fig. 3) could provide the correlation of conjugation length with the charge transport process. We reported that conjugation length of polymer electrets was able to manipulate transistor memory characteristics, using the polymer electrets of linear polystyrene para-substituted with π -conjugated oligofluorenes (**P10^L**).¹⁹ As can be observed from the positive and negative shifts in transfer curves of the OFET memories of Fig.4(a), trapping ability for both electrons

and holes enhanced and the memory windows are 99, 115, and 133 V for **P10^L** side chain with one, two and three fluorene units, respectively. The responding programming and erasing state currents of the devices are maintained over 100 cycles (Fig.4(b)), showing a good stability and fully reversibility. The longest fluorene side group with the lowest-lying LUMO level and the smallest band gap created a small barrier to facilitate the injection of electron from pentacene. Similar molecular design concept was employed in OFETs memory devices using n-type N,N-bis(2-phenylethyl)-perylene-3,4:9,10-tetracarboxylic diimide (BPE-PTCDI) and pendent polymer electret with one or three thiophene units in the side chain (**P11**).²⁰ The higher HOMO level (or smaller ionization potential) of **P11** with three connected π -conjugated thiophene rings facilitated more holes transfer from BPE-PTCDI layer to electret and resulted in a larger memory window of **P11** compared with that using **P10^L** with a similar conjugation length. This clearly indicates that the thiophene moiety is the stronger electron donor relative to fluorene which could enhance the ability to store the hole charges and thus lead to the larger memory window. As a result, tuning pendent conjugation length/strength could control the magnitude of memory windows.

3.1.3 Effect of architecture

Star-shaped polymers consisted of arms with macromolecule chain segments linking to a central core can have considerably different physical properties compared to their linear

analogues, owing to the close proximity of the arms within a single molecule. Our group first employed the three-armed star-shaped poly[(4-diphenylamino) benzyl methacrylate] (**P12**) as the charge storage electret for the BPE-PTCDI OFETs devices,²¹ which exhibited the large and irreversible negative threshold voltage shift in the transfer curves. It suggested that the electronic charges were transferred and permanently accumulate in the star-shaped **P12** gate electret due to the restricting region by the central nitrogen core of the star-shaped polymers with well-defined charge trapping elements as compared to that in linear analog. Interestingly, star-shaped **P12** electret-based OFETs memory devices showed nonvolatile write-many-read-many (WMRM) memory device behaviors obtained by applying different gate voltages, suggesting the multilevel data storage characteristics. Moreover, OFET memory device using the star-branched **P10**^S electrets with different arm numbers (three or four) showed the strong dependence of memory characteristics with the arm number.³² As the arm number increased, the OFET hole mobility and memory window were improved to 0.69 cm² V⁻¹ s⁻¹ and 19.75 V, with a high memory ratio of over 10⁸. The low dielectric constant and a larger free-volume distribution from molecular simulation of the large arm number led to the greater loaded electric field and resulted in a stronger hole storage and broaden memory window.

3.1.4 Effect of morphology

P-channel OFET memory devices incorporating the polystyrene-*block*-poly(4-vinylpyridine) (PS-*b*-P4VP; **P13**) charge trapping layer with the thickness-dependent micellar nanostructure exhibited tunable memory windows. The memory window increased substantially from 7.8 V for the device incorporating a 60 nm thick PS-*b*-P4VP layer to 21 V for that using a 27 nm thick layer.²² The P4VP core-PS shell micelles retained their cap-like structures, with the distance between them decreasing upon increasing the layer thickness of the **P13**. In contrast, the thickness of the PS shell along the in-plane direction decreased substantially, resulting in a decrease in the electron trapping ability of the **P13** layer and the memory window of the devices. Therefore, tuning the micellar nanostructure of the block copolymer thin film for charge-trapping represents a simple and effective way for optimizing the memory window.

3.1.5 Multilevel OFET memory devices

The majority of the aforementioned transistor memories that employed the polymer electret dielectric were limited to possess two-level memory characteristics. Historically, single cell devices were used to store one bit of information. However, the new generation nonvolatile memory stores more than one bit per cell with the multiple levels of electrical charge, named multilevel cell devices. The multilevel memory cell is a demonstrated technology, and it has become attractive due to the scaling limitations of lithography

technology. We have used the star-branched polymer electrets to achieve the multilevel memory behaviors, as described in section 3.1.3. There are some other examples reported in the literature, as described in the following. Guo et. al. demonstrated the five-level storage OFET memory devices using **P5** or **P9** modifying SiO₂ layers,²³ as shown in Fig. 5. These characteristics were believed to originate from the use of optical and electrical organic semiconductor that performs the appropriate writing and erasing operations. However, the operating voltage is -60 V and the program voltage for the highest level was -200 V, which limited their practical applications. Shang et al. realized a low-voltage multilevel OFET storage cell using high-*k* Al₂O₃ thin film modified by **P9** electret under a positive gate biases assisted with light illumination.²⁴ Charges could be stored over 1×10⁴ s and the states were clearly distinguished after 1×10⁴ endurance cycles within the low working voltage bias pulses of ±9 V.

Baeg, Noh and coworkers first demonstrated inkjet-printed dodecyl-substituted thienylenevinylene-thiophene copolymer (PC12TV12T)-based OFET memory devices using the **P5** or **P6** chargeable electrets and high-*k* blocking gate dielectric poly(vinylidene fluoride trifluoroethylene) (P(VDF-TrFE)) in a top-gate/bottom-contact (TGBC) device architecture.²⁵ The above OFET exhibited a flash memory with a reduced contact resistance for charge injection and a decrease in the current crowding effect to show a large memory window in a short amount of switching time. By applying suitable gate biases with various ranges, various

discrete memory levels (two bits per cell) for realizing each of states of “00”, “01”, “10”, and “11” was addressed. The device with the **P6** electret exhibited better memory characteristics than that using the **P5** due to the lower injection barrier in a more extended π -conjugation length of the **P6** electret.

3.2 Donor-acceptor type main-chain polyimide electret

Field-induced intramolecular charge transfer (ICT) behavior of D-A type polymeric materials could enhance the charge storage ability as the electrets for high performance OFET memory applications.² Especially, D-A polyimides (PI) materials have the advantages of homogeneity, thermal stability, and chemical resistance, which were widely used for resistor-type memory devices in recent years.^{2,36,37} The variety of PI structures reported so far is shown in Fig.6 and the corresponding electronic properties are collected in Table 2.

Our group reported the nonvolatile memory characteristics of n-type BPE-PTCDI based OFET devices using the PI electrets of poly[2,5-bis(4-aminophenylenesulfanyl)selenophene-hexafluoroisopropylidenedipthalimide] (**P14**), and poly [2,5-bis(4-aminophenylenesulfanyl)-thiophene-hexafluoroisopropylidenedipthalimide] (**P15**). The OFET memory device based on **P14** with a strong electron-rich selenophene cyclic ring exhibited the highest field effect mobility due to the formation of the large grain size of the BPE-PTCDI semiconductor

nanowire.²⁶ Furthermore, **P14**-based device also showed the larger memory window of 63 V because the highest HOMO energy level of **P14** and high electric field facilitated the charges efficiently transferring from BPE-PTCDI and trapping in the **P14** electret. Moreover, high dielectric PI electret, consisting of electron-donating 4,4'-diamino-4''-cyanotriphenylamine with different electron-accepting 2,2-bis(3,4-dicarboxyphenyl)hexafluoropropane diphthalic anhydride (6FDA, **P16**) and 3,3',4,4'-benzophenonetetracarboxylic dianhydride (BTDA, **P17**) and 3,3',4,4'-diphenylsulfonetetracarboxylic dianhydride (DSDA, **P18**), were also employed for pentacene-based OFET memory device.²⁷ The dielectric constants of **P16**, **P17** and **P18** were 3.70, 3.44, and 3.52, respectively, higher than those (~3) of common PI. Among these three PI electrets with different linkages in anhydride discussed here, the OFET device using the **P16** electret exhibited the highest mobility of $0.5 \text{ cm}^2 \text{ V}^{-1} \text{ s}^{-1}$ due to the formation of a pentacene film of large grain size by the hydrophobic surface. A more twisted conformation of **P16** hindered the charge transfer back to the ground state and trapped the charges deeply, leading to a highest memory window, as shown in Fig.7. Similar characterization was explored in the OFET devices based on the PI electrets (**P19**, **P20** and **P21**) made from 4,4'-diamino-4''-methyltriphenylamine (AMTPA) electron-donating moieties or further containing pendent polycyclic arenes of naphthalene (APAN) and pyrene (APAP), respectively, individually polyimidized with 6FDA electron-accepting moieties.²⁸ Among the three electrets, the aromatic pyrene in **P21**-based OFET memory

device successfully maintained the programmed state without significant decay for over 10^4 s and enhanced the charge trapping ability, resulting in the large memory window of 40.63 V.

OFET memory devices employing functional PI electrets that comprise identical phenylene sulfide electron donor coupled with three building blocks based on gradually increasing electron-accepting ability (**P22**, **P23** and **P24**) to manipulate the memory characteristics.²⁹ The **P22** electret with the prominent electron-donating ability exhibited a hole trapping-only behavior, resulting in an inerasable write-once-read-many (WORM)-type memory. However, the programmed transfer curves of the devices based on the **P23** and **P24** electrets were easily erased, showing flash-type memory characteristics. The induced electron in the BPE-PTCDI semiconductor layer was likely to be captured by the accepting moiety of the **P23** and **P24** electret, while applying an erasing pulse. Considering the facilitation of the charge transfer complex of **P23** and **P24**, the transferred electrons neutralized the stored holes in the electrets and completed the erasing actions. It indicated that the performance of OFET memory devices could be modulated by controlling the charge transfer features of the PI chargeable electrets.

3.4 Polymer composite electrets

Polymer composites by embedding the functional moieties into polymer matrix as charge trapping layer in OFET memory devices have recently attracted considerable interest.¹ A further enhancement of memory window was realized by blending the polymer layer with

well-known semiconducting molecules, such as graphene oxide (**GO**),³⁴ tetrathiafulvalene (**TTF**),³⁰ ferrocene (**Fc**),^{30, 35} 6,6-phenyl-C61-butyric acid methyl ester (**PCBM**),^{31, 32, 35} 1-aminopyrene (**APy**),³³ 6,13-bis(triisopropylsilyl-ethynyl)pentacene (**TIPS-pen**),³⁵ etc. Fig. 8 summarizes the structures and Table 4 shows the memory parameters of the reported polymer composites as the charge trapping electrets

High performance OFET memory element with electron-donor composites as buffer dielectric were presented by Liu and coworkers,³⁰ using the organic molecules (such as **TTF** and **Fc**) as donors blended into polymer matrix (such as polycarbonate (**PC**; **P25**), poly(ethylene oxide) (**PEO**; **P26**), **P5** and **P9**). For such copper phthalocyanine (**CuPc**)-based OFET memory devices using polymer/donor composites as charge trapping electret, charge tunneling through the insulator polymer on organic donor was possible when the **CuPc** (function as acceptor here) contacted with a strong donor molecule. Therefore, the carriers were generated and the device exhibited a sharp increase in conductivity/memory switching after the charge transfer. Pentacene-based OFET-type nonvolatile memory using **P7** or **P10^S:PCBM** nanocomposite electrets were demonstrated,^{31,32} with a low operating voltage owing to the high capacitance of the dielectric film and the high electron-withdrawing property of **PCBM**.³¹ Memory devices utilizing star-branched **P10^S** with different arm numbers have already discussed in section 3.1.2.³² The device memory performance was further improved using the blend electret of **P10^S:PCBM**, due to the facilitated charge

transfer between pentacene and D-A hybrid electret. In the following, we explored the OFET memory devices using the n-type BPE-PTCDI active semiconductor layer using the composite electrets of **P12** pendent donor polymer with three semiconducting small molecules (i.e., **PCBM** acceptor as well as **TIPS-pen** and **Fc** donors).³⁵ In the device using **P14:PCBM** electret, it changed its memory feature from a WORM type to flash type as the **PCBM** content increased and could be operated repeatedly. However, the memory characteristics showed a flash and WORM type, respectively, using donor/donor electrets **TIPS-pen:P12** and **Fc:P14**. The slightly higher LUMO barrier (1.10 eV) between BPE-PTCDI and **TIPS-pen** than that of the **PCBM** case (0.51 eV) resulted in the tunneling of the induced electrons through the **P12** into the **TIPS-pen** for recombining the trapped holes as flash-type memory behavior. The irreversible behavior of device using **P14:Fc** composite electret was attributed to the larger gap of the LUMO energy level (2.3 eV) between BPE-PTCDI and **Fc** than those between BPEPTCDI and **TIPS-pen** or **PCBM** for the electron trapping.

Recently, the construction of the composite electret films in which layers of hydrogen-bonded small molecule components are embedded within electrically-insulated polymers was reported by our group.^{33,34} Green hybrid electrets of sugar-based block copolymer maltoheptaose-*block*-polystyrene (MH-*b*-PS; **P27**) and hydrogen-bonded **APy** to the MH moieties of **P27**.³³ Via the solvent annealing, the orientation of the ordered MH

nanodomains was well controlled in the PS matrix, including random spheres, vertical cylinders, and well-ordered horizontal cylinders. The hysteresis loops and memory window was significantly improved from the random sphere structures to horizontal cylinders under a fixed loading ratio because of the larger interfacial area for the charge trapping. The optimized device using the horizontal cylinders of the supramolecular **P27:Apy** composite electrets exhibited the excellent memory characteristics of a wide memory window (52.7 V), retention time longer than 10^4 s with a high memory ratio of $>10^5$, and stable reversibility over 200 cycles. Besides, the hydrogen bonding interaction effectively disperses **GO** sheets in the high- k poly(methacrylic acid) (**P28**) matrix, leading to the manipulation on memory characteristics with the GO composition.³⁴ The fabricated OFET memory devices have a low operation voltage, a large threshold voltage shift of 5.3~9.4V, a long retention ability of up to 10^4 s, a good stress endurance of at least 100 cycles, and the bending stability.

4 Conclusions and outlook

We have reviewed the representative and promising polymer electrets as the charge trapping layer for OFET memory devices. Rational design on backbone of repeating units as well as interaction between guest additive and host matrix inside the polymer composites is of utmost import for further development of OFET memories. Several factors for molecular design are summarized to vary the performance of the memory devices (Fig. 9), including the

surface polarity, conjugation length, architecture, and donor/acceptor strength, and interfacial energy barrier. Polymer electrets with a longer conjugation length in side-chain moieties, more hydrophobic and smaller interface energy barrier could have efficient charge trapping for achieving the larger memory window of the device.

The basic requirements of these intrinsic charge trapping properties for the polymer charge storage materials include: (1) thick enough and high thermal stability hydrophobic polymer charge trapping layer to avoid the charge dissipation loss; (2) solution-processed smooth polymer electrets to provide a well-defined interface for the formation of high quality and high mobility organic semiconductor films; (3) suitable HOMO/LUMO energy levels and architecture of electret materials relative to organic semiconductors to ensure the hole/electron charge trapping condition and stability; (4) future memory trend for processor design is that with lower working voltage comes lower overall power consumption and widespread use of nonvolatile memories requires high operation reliability and excellent data retention; (5) integration of other organic electronic or optoelectronic devices. The above guidelines could help on developing polymer electrets for high performance nonvolatile memory devices toward practical applications.

Acknowledgement

This work was supported by Ministry of Science and Technology of Taiwan.

References

1. P. Heremans, G. H. Gelinck, R. Muller, K.-J. Baeg, D.-Y. Kim and Y.-Y. Noh, *Chem. Mater.*, 2011, **23**, 341.
2. Q.-D. Ling, D.-J. Liaw, C. Zhu, D. S.-H. Chan, E.-T. Kang and K.-G. Neoh, *Prog. Polym. Sci.*, 2008, **33**, 917.
3. W. L. Leong, N. Mathews, B. Tan, S. Vaidyanathan, F. Doetz and S. Mhaisalkar, *J. Mater. Chem.*, 2011, **21**, 5203.
4. J.-S. Lee, *J. Mater. Chem.*, 2011, **21**, 14097.
5. Y. Guo, G. Yu and Y. Liu, *Adv. Mater.*, 2010, **22**, 4427.
6. S.-T. Han, Y. Zhou and V. A. L. Roy, *Adv. Mater.*, 2013, **25**, 5425.
7. B. M. Dhar, R. Oezguen, T. Dawidczyk, A. Andreou and H. E. Katz, *Mater. Sci. Eng. R*, 2011, **72**, 49.
8. R. C. G. Naber, K. Asadi, P. W. M. Blom, D. M. de Leeuw and B. de Boer, *Adv. Mater.*, 2010, **22**, 933.
9. D. P. Erhard, D. Lovera, C. von Salis-Soglio, R. Giesa, V. Altstaedt and H.-W. Schmidt, *Adv. Polym. Sci.*, 2010, **228**, 155.
10. H. E. Katz, X. M. Hong, A. Dodabalapur and R. Sarpeshkar, *J. Appl. Phys.*, 2002, **91**, 1572.
11. T. B. Singh, N. Marjanovic, G. J. Matt, N. S. Sariciftci, R. Schwodiauer and S. Bauer, *Appl. Phys. Lett.*, 2004, **85**, 5409.
12. B. Mukherjee and M. Mukherjee, *Org. Electron.*, 2009, **10**, 1282.
13. K. J. Baeg, Y. Y. Noh, J. Ghim, S. J. Kang, H. Lee and D. Y. Kim, *Adv. Mater.*, 2006, **18**, 3179.
14. K.-J. Baeg, Y.-Y. Noh, J. Ghim, B. Lim and D.-Y. Kim, *Adv. Funct. Mater.*, 2008, **18**, 3678.
15. S. C. Lim, S. H. Kim, J. B. Koo, J. H. Lee, C. H. Ku, Y. S. Yang and T. Zyung, *App. Phys. Lett.*, 2007, **90**, 173512.
16. T.-D. Tsai, J.-W. Chang, T.-C. Wen and T.-F. Guo, *Adv. Funct. Mater.*, 2013, **23**, 4206.
17. M. Debucquoy, M. Rockele, J. Genoe, G. H. Gelinck and P. Heremans, *Org. Electron.*, 2009, **10**, 1252.
18. B.-L. Yeh, Y.-H. Chen, L.-Y. Chiu, J.-W. Lin, W.-Y. Chen, J.-S. Chen, T.-H. Chou, W.-Y. Chou, F.-C. Tang and H.-L. Cheng, *J. Electrochem. Soc.*, 2011, **158**, H277.
19. J.-C. Hsu, W.-Y. Lee, H.-C. Wu, K. Sugiyama, A. Hirao and W.-C. Chen, *J. Mater. Chem.*, 2012, **22**, 5820.
20. Y.-H. Chou, S. Takasugi, R. Goseki, T. Ishizone and W.-C. Chen, *Polym. Chem.*, 2014,

- 5, 1063.
21. Y.-C. Chiu, C.-L. Liu, W.-Y. Lee, Y. Chen, T. Kakuchi and W.-C. Chen, *NPG Asia Mater.*, 2013, **5**, e35.
 22. C.-M. Chen, C.-M. Liu, M.-C. Tsai, H.-C. Chen and K.-H. Wei, *J. Mater. Chem. C*, 2013, **1**, 2328.
 23. Y. Guo, C.-a. Di, S. Ye, X. Sun, J. Zheng, Y. Wen, W. Wu, G. Yu and Y. Liu, *Adv. Mater.*, 2009, **21**, 1954.
 24. L. Shang, Z. Ji, H. Wang, Y. Chen, X. Liu, M. Han and M. Liu, *IEEE Electron Dev. Lett.*, 2011, **32**, 1451.
 25. K.-J. Baeg, D. Khim, J. Kim, B.-D. Yang, M. Kang, S.-W. Jung, I.-K. You, D.-Y. Kim and Y.-Y. Noh, *Adv. Funct. Mater.*, 2012, **22**, 2915.
 26. Y.-H. Chou, N.-H. You, T. Kurosawa, W.-Y. Lee, T. Higashihara, M. Ueda and W.-C. Chen, *Macromolecules*, 2012, **45**, 6946.
 27. Y.-H. Chou, H.-J. Yen, C.-L. Tsai, W.-Y. Lee, G.-S. Liou and W.-C. Chen, *J. Mater. Chem. C*, 2013, **1**, 3235.
 28. A.-D. Yu, T. Kurosawa, M. Ueda and W.-C. Chen, *J. Polym. Sci. Polym. Chem.*, 2014, **52**, 139.
 29. A.-D. Yu, W.-Y. Tung, Y.-C. Chiu, C.-C. Chueh, G.-S. Liou and W.-C. Chen, *Macromol. Rapid Commun.*, 2014, **35**, 1039.
 30. W. Wu, H. Zhang, Y. Wang, S. Ye, Y. Guo, C. Di, G. Yu, D. Zhu and Y. Liu, *Adv. Funct. Mater.*, 2008, **18**, 2593.
 31. K.-J. Baeg, D. Khim, D.-Y. Kim, S.-W. Jung, J. B. Koo and Y.-Y. Noh, *Jpn. J. Appl. Phys.*, 2010, **49**, 05EB01.
 32. Y.-C. Chiu, T.-Y. Chen, C.-C. Chueh, H.-Y. Chang, K. Sugiyama, Y.-J. Sheng, A. Hirao and W.-C. Chen, *J. Mater. Chem. C*, 2014, **2**, 1436.
 33. Y.-C. Chiu, I. Otsuka, S. Halila, R. Borsali and W.-C. Chen, *Adv. Funct. Mater.*, 2014, **24**, 4240.
 34. Y.-H. Chou, Y.-C. Chiu and W.-C. Chen, *Chem. Comm.*, 2014, **50**, 3217.
 35. Y.-C. Chiu, T.-Y. Chen, Y. Chen, T. Satoh, T. Kakuchi and W.-C. Chen, *ACS Appl. Mater. Interface*, 2014, **6**, 12780.
 36. C.-L. Liu and W.-C. Chen, *Polym. Chem.*, 2011, **2**, 2169.
 37. T. Kurosawa, T. Higashihara and M. Ueda, *Polym. Chem.*, 2013, **4**, 16.

Table 1 OFETs memory device performance based on pendent polymer electrets

Electret	Organic semiconductor	Memory window/V	Memory ratio/V	$\mu/\text{cm}^2 \text{V}^{-1} \text{s}^{-1}$	Ref.
Effect of hydrophobic/hydrophilic pendent groups					
P1	PTPTP	30	10^3	0.02	10
P1	F15-NTCDI	30	10^1	0.001	10
P2	PTPTP	95	10^3	10^{-4}	10
P2	F15-NTCDI	40	10^1	10^{-5}	10
P3	PCBM	14	10^4	0.09	11
P3	PbPc	10	10	–	12
P3	pentacene	–	10^5	0.07	14
P3	pentacene	18.5~35.7	10^2	–	16
P3	pentacene	–	3.7	10^3	13
P4	pentacene	90	10^5	0.5	13
P4	pentacene	26	10^5	0.35	14
P4	pentacene	12	10^6	0.8	17
P5	pentacene	22.1	10^5	0.26	14
P6	pentacene	27.8	10^6	0.61	14
P7	pentacene	17	10^5	0.21	14
P7^a	pentacene	2~41	$10^3\sim 10^5$	0.04~0.17	15
P8	pentacene	21	10^5	0.12	14
P9	pentacene	3.1	10^3	–	18
Effect of π -conjugated length					
P10^{Lb}	pentacene	99~133	$10^5\sim 10^6$	0.04~0.47	19
P11	BPE-PTCDI	49, 81	$10^2\sim 10^3$	$(2.2\sim 3.6) \times 10^{-3}$	20
Effect of architecture					
P12^c	BPE-PTCDI	36.5	10^5	0.02	21
P12^c	pentacene	54	10^6	0.27	21
P10^{Sc}	pentacene	7.80~19.75	10^8	0.34~0.69	32
Effect of morphology					
P13	pentacene	7.8~21.1	10^5	0.1~0.46	22
Multilevel memory					
P5^d	pentacene	114	10^6	0.5	23
P5^d	CuPc	128	10^4	0.01	23

P9	pentacene	123	10^6	0.5	23
P9	CuPc	113	10^4	0.01	23
P9	pentacene	6	10^7	0.3	24
P5^c	PC12TV12T	5~34	10^8	0.11	25
P6^c	PC12TV12T	11~92	10^7	0.061	25

^acrosslinking polymer

^blinear polymer

^cstar-branched polymer

^dunder light illumination

^etop-gate bottom contact device structure

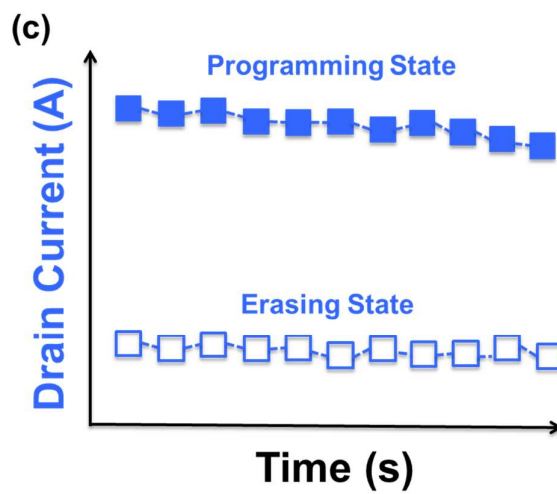
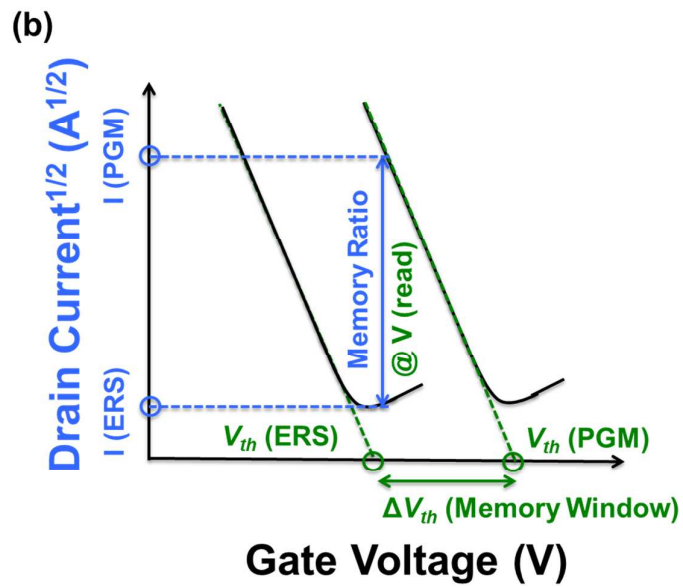
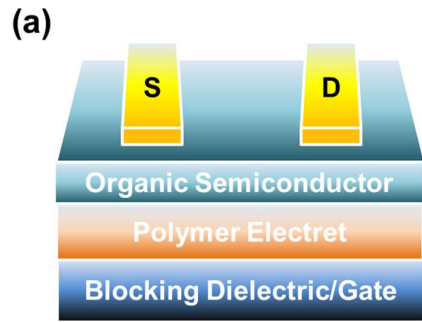
Table 2 OFET memory device performance using polyimides electrets

Electret	Organic semiconductor	Memory window/V	Memory ratio/V	$\mu/\text{cm}^2 \text{V}^{-1} \text{s}^{-1}$	Ref.
P14	BPE-PTCDI	63	10^3	3.6×10^{-3}	26
P15	BPE-PTCDI	41	10^3	2.4×10^{-3}	26
P16	pentacene	84	10^6	0.5	27
P17	pentacene	30	10^5	0.09	27
P18	pentacene	65	10^5	0.21	27
P19	BPE-PTCDI	18.05	10^4	7.6×10^{-3}	28
P20	BPE-PTCDI	33.71	10^4	5×10^{-3}	28
P21	BPE-PTCDI	40.63	10^4	8.2×10^{-3}	28
P22	BPE-PTCDI	64.39	10^5	5.7×10^{-3}	29
P23	BPE-PTCDI	61.22	10^4	1.3×10^{-3}	29
P24	BPE-PTCDI	81.49	10^4	6×10^{-4}	29

Table 3 OFET memory device performance using polymer composites as the charge storage electret.

Electret	Organic semiconductor	Memory window/V	Memory ratio/V	$\mu/\text{cm}^2 \text{V}^{-1} \text{s}^{-1}$	Ref
P9:TTF	CuPc	173	75	0.027	30
P5:Fc	CuPc	58	500	3.73×10^{-4}	30
P9:Fc	CuPc	155	2×10^3	2.21×10^{-3}	30
P25:Fc	CuPc	156	2×10^4	3.71×10^{-4}	30
P26:Fc	CuPc	90	3×10^4	4.38×10^{-4}	30
P7:PCBM	pentacene	20	10^4	0.2~0.3	31
P10^{Star}:PCBM	pentacene	30.41~35.59	10^6	0.73~1.04	32
P27:APy	pentacene	52.7	52.7	0.42~0.57	33
P28:GO	TIPS-pen	1~9.4	$(1.3\sim 4.2) \times 10^4$	$(4.4\sim 6.2) \times 10^{-3}$	34
P12:PCBM	BPE-PTCDI	17.89~30.96	10^3	0.0025	35
P12:TIPS-pen	BPE-PTCDI	27.95	10^3	0.0027	35
P12:Fc	BPE-PTCDI	0.81	10^4	0.0332	35

^astar-branched polymer



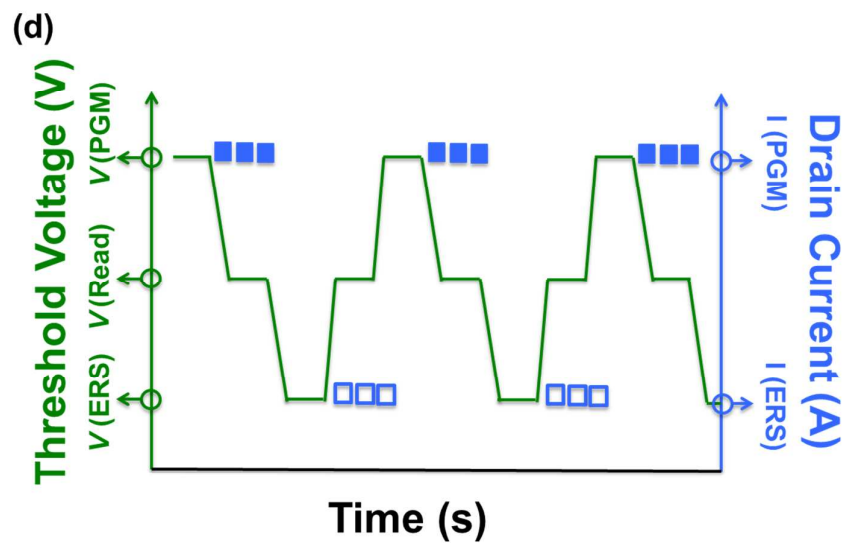


Fig. 1 (a) Schematic configuration of OFET memory devices. (b) $I_d^{1/2}$ vs V_g curve under applied voltage bias that can determine the memory window and memory ratio. (c) Retention time and (d) endurance cycles on OFET memory devices.

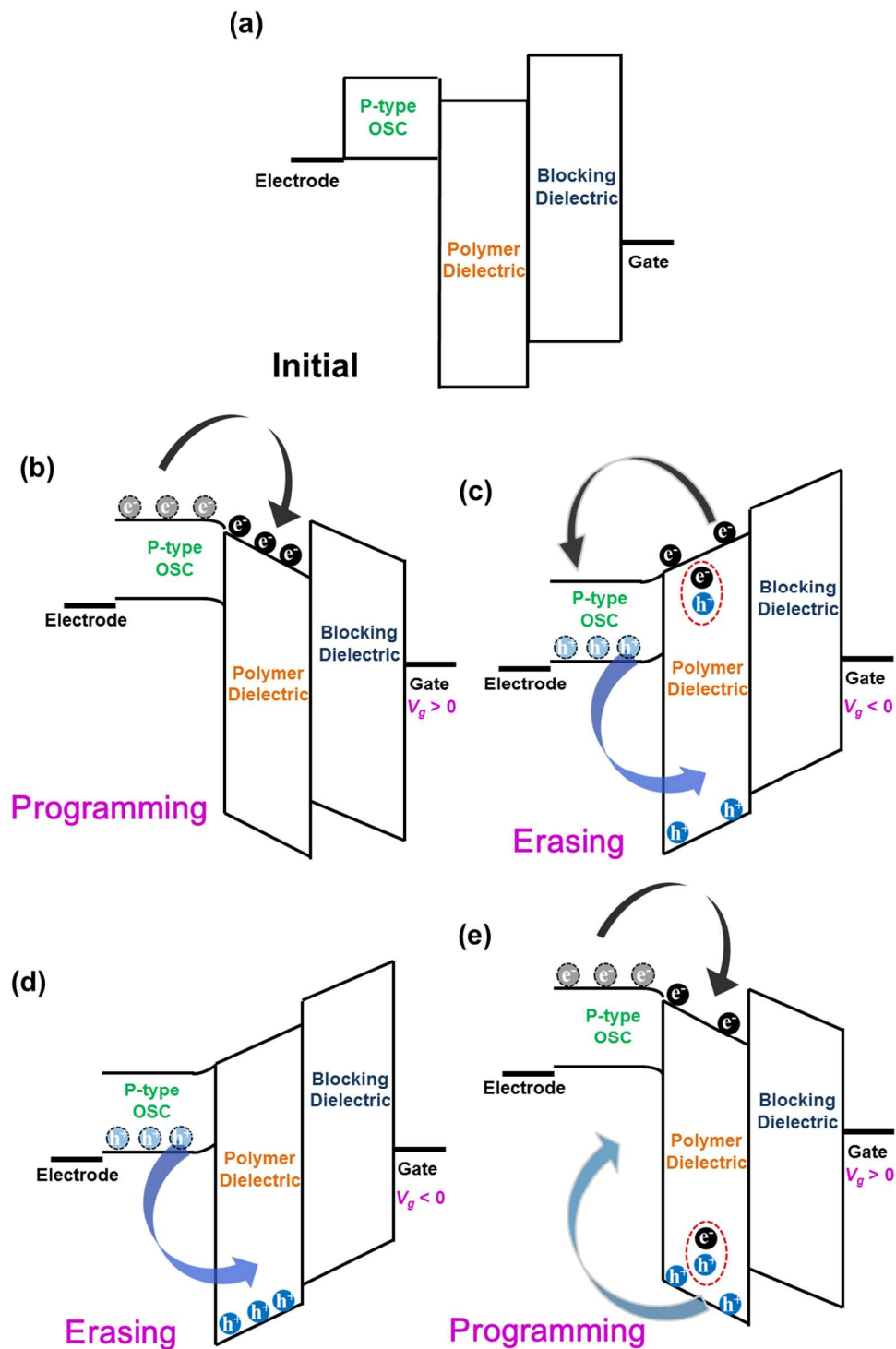


Fig. 2 P-type OFET memory devices operation: (a) flat-band condition, (b) hole trapping (PGM mode), (c) electron trapping (ERS mode), (d) hole detrapping and recombination with electron (ERS mode) and (e) electron detrapping and recombination with hole (PGM mode).

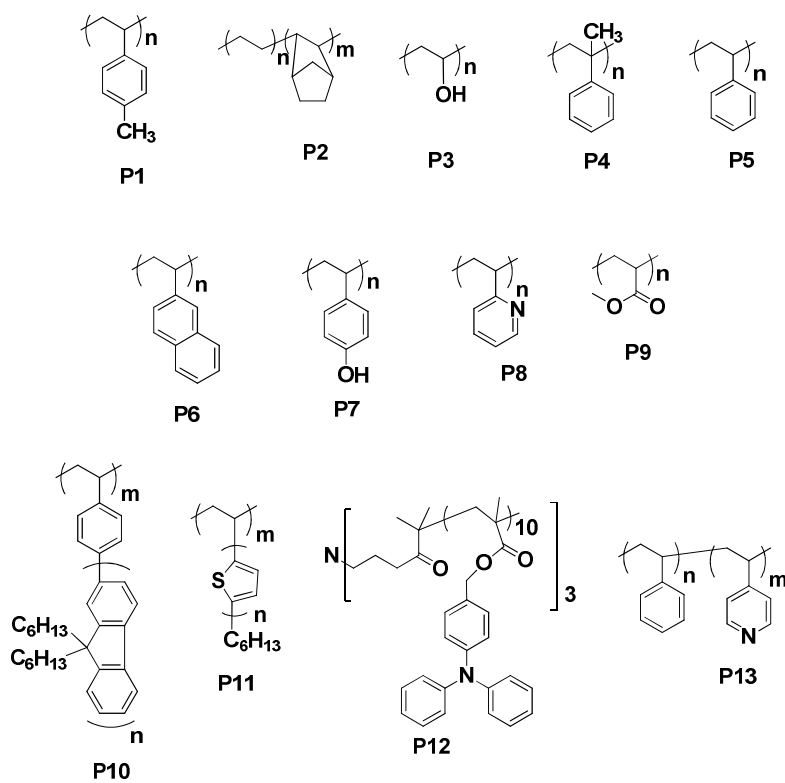


Fig. 3 Chemical structures of the polymer electrets with the pendent charge storage moiety.

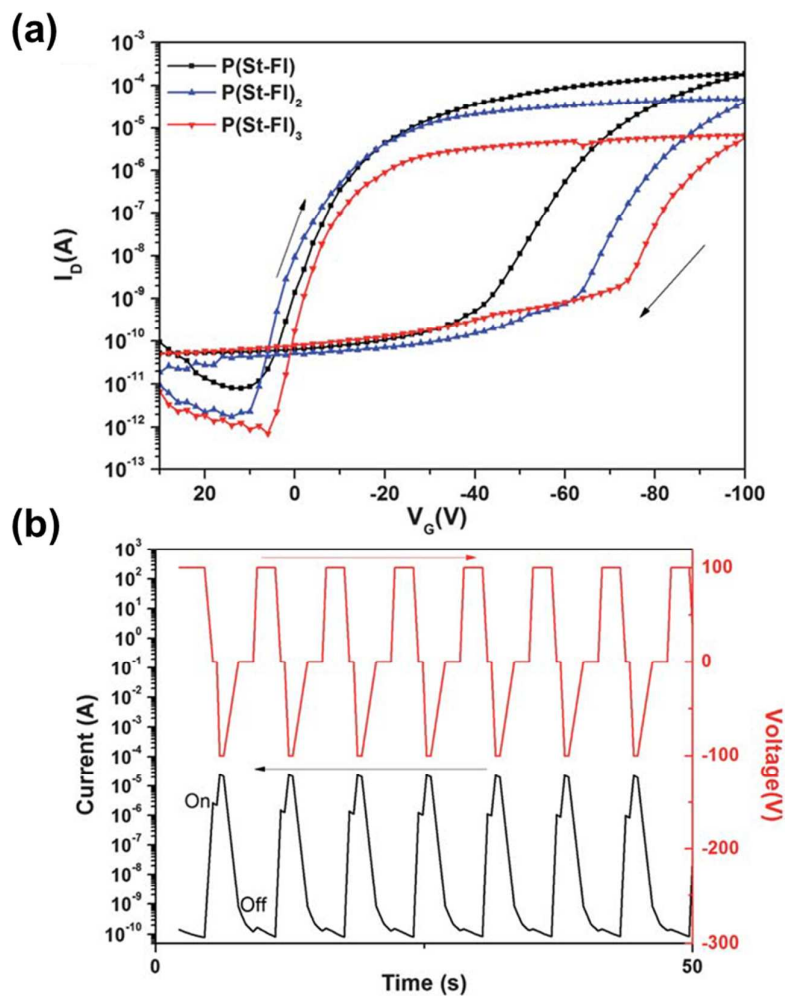


Fig. 4 (a) Transfer characteristics and (b) reversible switching for programming and erasing states of pentacene-based OFET memory devices using the **P19** electret. Reproduced from Ref. 27 with permission from The Royal Society of Chemistry.

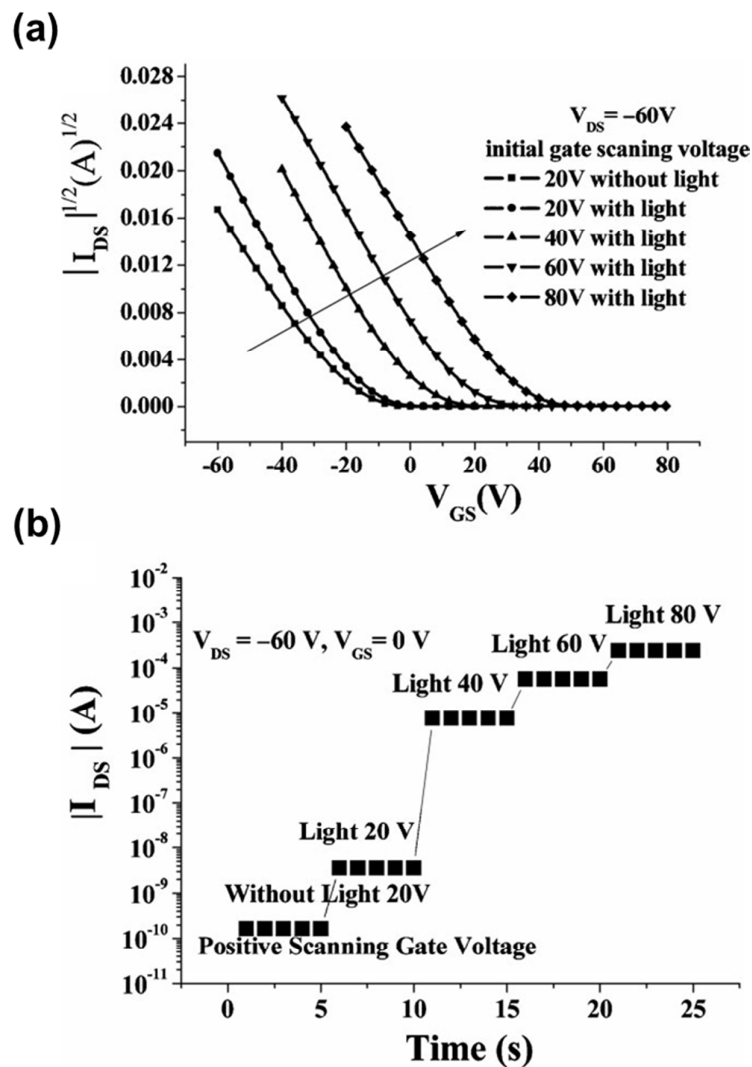


Fig. 5 Transfer characteristics of OFETs memory devices based on P5 electret under a light-assisted programming: (a) (drain current)^{1/2} vs gate voltage and (b) the corresponding different current levels at gate voltage of 0 V and drain voltage of -60 V. Reproduced from Ref. 23 with permission from Wiley-VCH.

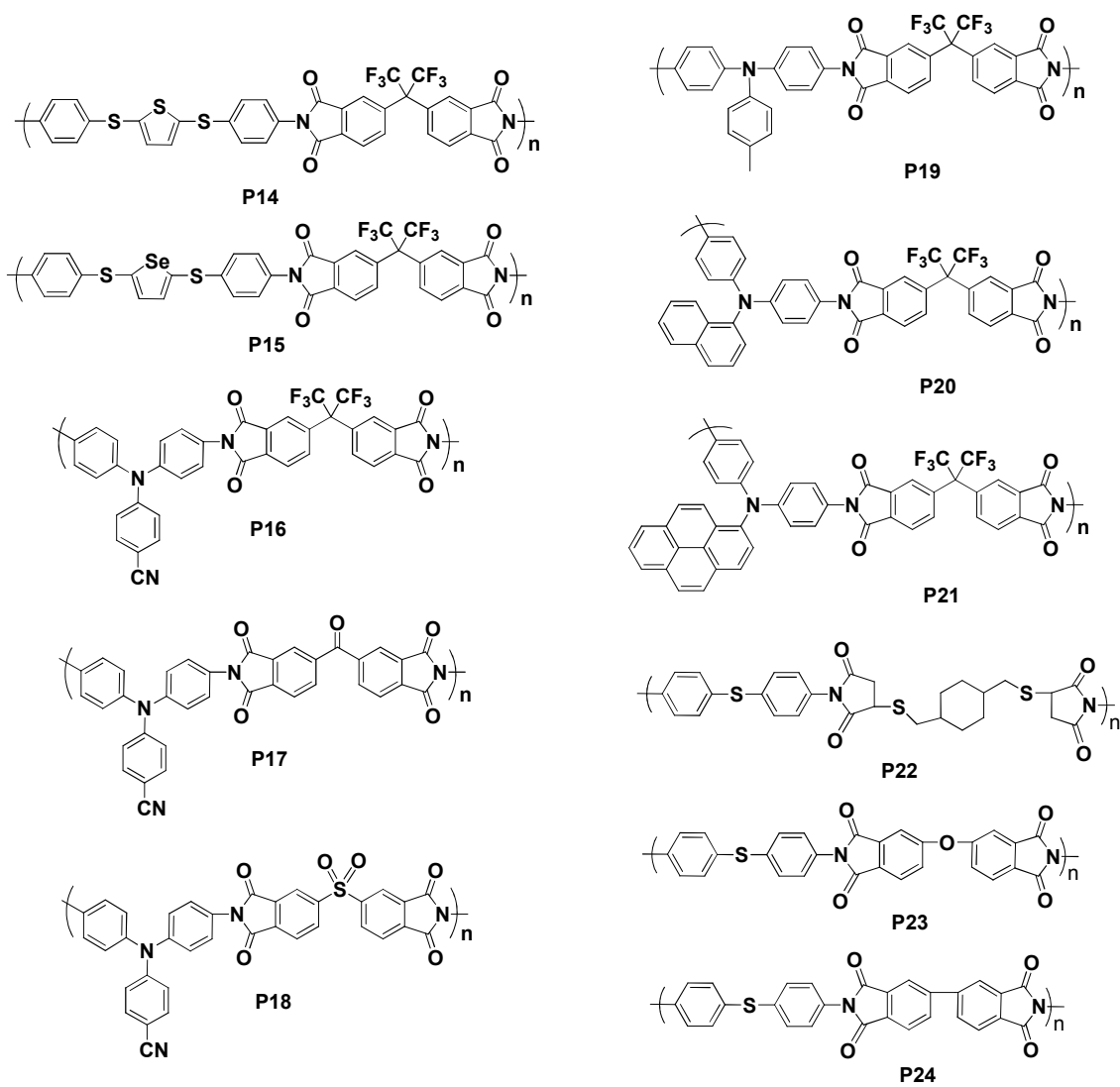


Fig. 6 Chemical structures of the donor-acceptor type main chain polyimides electrets.

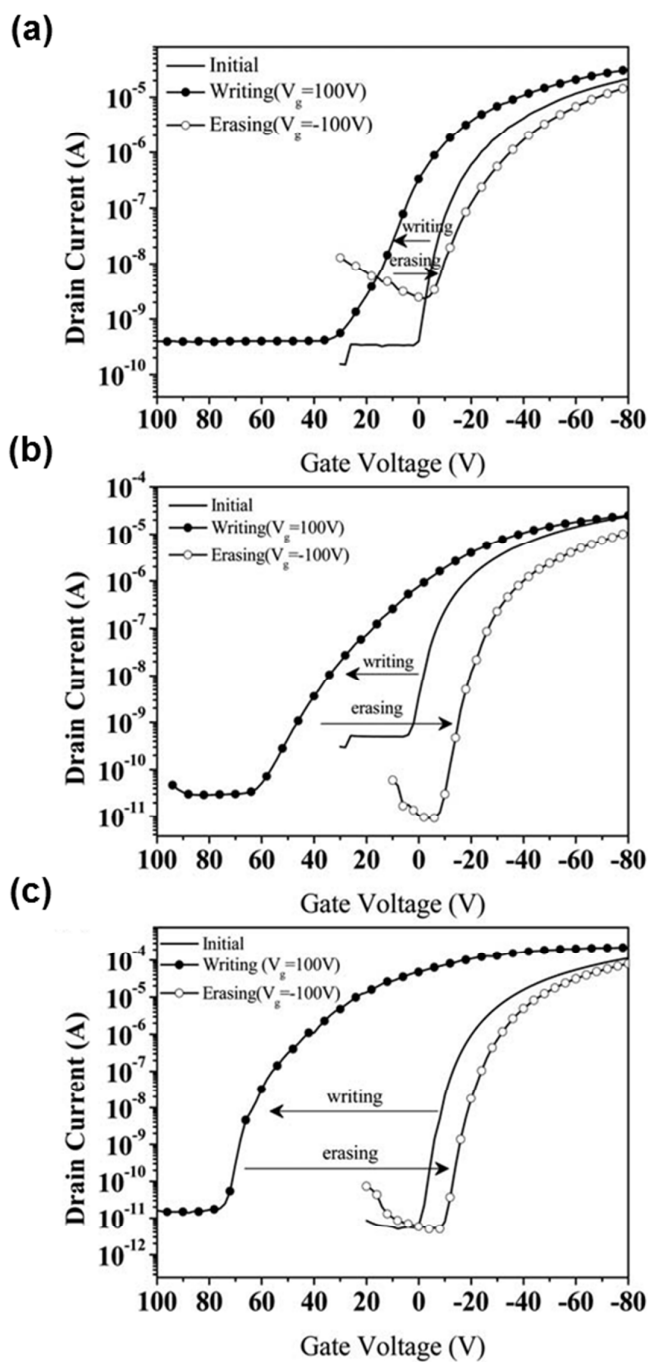


Fig. 7 Reversible shift in transfer plots of the pentacene-based OFET memory devices based on (a) **P17**, (b) **P18**, and (c) **P16** electret. Reproduced from Ref. 34 with permission from The Royal Society of Chemistry.

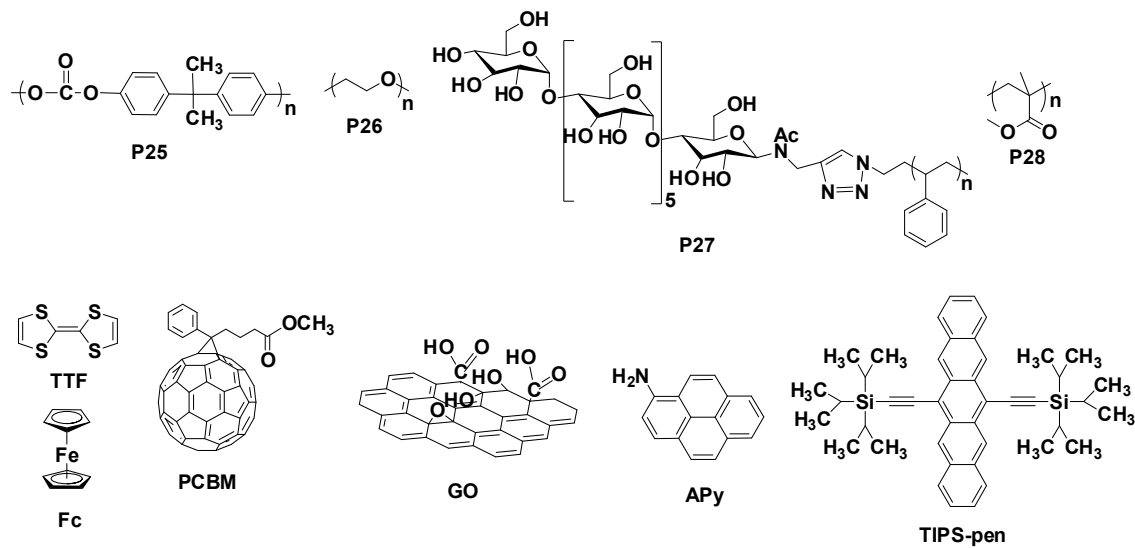


Fig. 8 Chemical structures of materials used in polymer composites as charge storage electrets.

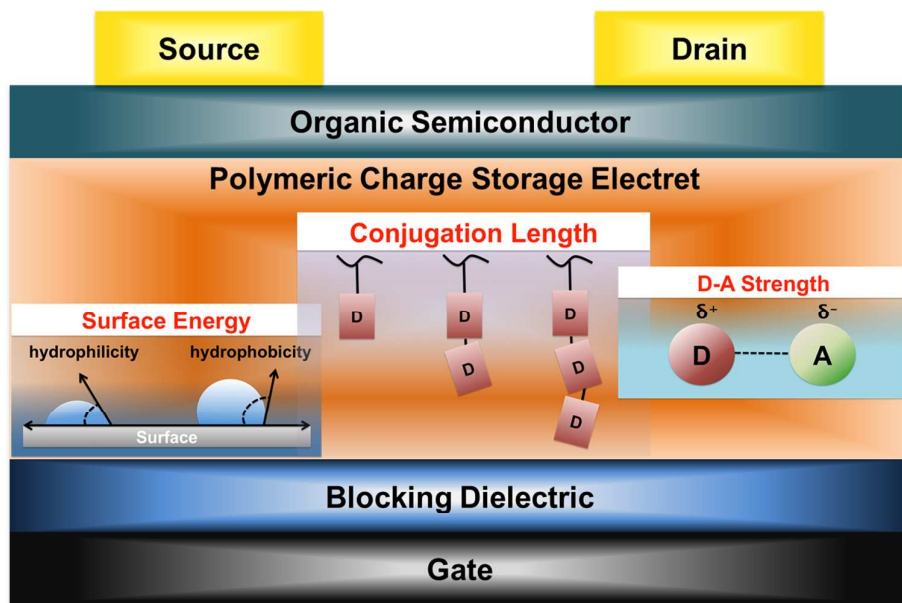


Fig. 9 Structural factors on the polymer electrets for the performance of OFET memories.